

Traffic Engineering in Large-scale Networks with Generalizable Graph Neural Networks

Fangtong Zhou, Xiaorui Liu, Ruozhou Yu, Guoliang Xue

Abstract—Traffic engineering (TE) in large-scale computer networks has become a fundamental yet challenging problem, owing to the swift growth of global-scale cloud wide-area networks or backbone low-Earth-orbit satellite constellations. To address the scalability issue of traditional TE algorithms, learning-based approaches have been proposed, showing potential of significant efficiency improvement over state-of-the-art methods. Nevertheless, the intrinsic limitations of existing learning-based methods hinder their practical application: they are not generalizable across diverse topologies and network conditions, incur excessive training overhead, and do not respect link capacities by default.

This paper proposes TELGEN, a novel TE algorithm that learns to solve TE problems efficiently in large-scale networks, while achieving superior generalizability across diverse network conditions. TELGEN is based on the novel idea of transforming the problem of “predicting the optimal TE solution” into “predicting the optimal TE algorithm”, which enables TELGEN to learn and efficiently approximate the end-to-end solving process of classical optimal TE algorithms. The learned algorithm is agnostic to the exact network topology or traffic patterns, and can efficiently solve TE problems given arbitrary inputs and generalize well to unseen topologies and demands.

We trained and evaluated TELGEN on random and real-world networks with up to 5000 nodes and 10^6 links. TELGEN achieved less than 3% optimality gap while ensuring feasibility in all cases, even when the test network had up to $20\times$ more nodes than the largest in training. It also saved up to 84% solving time than classical optimal solver, and could reduce training time per epoch and solving time by 2–4 orders of magnitude than latest learning algorithms on the largest networks.

Index Terms—Traffic Engineering, Network Optimization, Learn-to-Optimize, Graph Neural Network, Machine Learning

I. INTRODUCTION

Traffic Engineering (TE) is becoming increasingly crucial amid the exponential growth in Internet traffic. With the help of software-defined networking (SDN), TE sits at the center of network management, supporting billions of applications

Zhou, Liu, Yu ({fzhou, xliu96, ryu5}@ncsu.edu) are with the Department of Computer Science at the North Carolina State University, Raleigh, NC, 27606, USA. Xue (xue@asu.edu) is with the School of Computing and Augmented Intelligence at the Arizona State University, Tempe, AZ, 85287, USA. The research of Zhou and Yu was supported in part by NSF grants 2045539 and 2433966. The research of Xue was sponsored in part by the Army Research Laboratory and was accomplished under Cooperative Agreement Number W911NF-23-2-0225. The views and conclusions contained in this document are those of the authors and should not be interpreted as representing the official policies, either expressed or implied, of the Army Research Laboratory or the U.S. Government. The U.S. Government is authorized to reproduce and distribute reprints for Government purposes notwithstanding any copyright notation herein.

© 20xx IEEE. Personal use of this material is permitted. Permission from IEEE must be obtained for all other uses, in any current or future media, including reprinting/republishing this material for advertising or promotional purposes, creating new collective works, for resale or redistribution to servers or lists, or reuse of any copyrighted component of this work in other works.

and users for achieving the best performance and experience. Usually, TE is implemented by a central controller that has a global view of the network and can make informed decisions about routing and traffic splitting to optimize traffic [26].

With the emergence of large-scale and dynamic networks, classical TE faces fundamental challenges in terms of scalability, responsiveness and performance. Wide-area networks (WANs), such as Cloud WAN or low-Earth-orbit (LEO) satellite backbone networks, typically consist of hundreds to thousands of nodes and tens of thousands to millions of links. These networks present prohibitively large TE problem sizes that existing optimization-based algorithms cannot catch up with. Some networks also exhibit frequent topology changes and dynamic demand variations, which requires repeated and frequent solving of the TE problem at small timescales [39]. State-of-the-art linear program (LP) solvers, widely used to solve TE problems, can lead to up to cubic complexity in the number of links and traffic flows, which is prohibitive for modern network sizes. Some decomposition-based algorithms have been proposed [2], [27], but can only utilize limited CPU parallelism for moderate speed-up with no asymptotic improvement, and usually have suboptimal performance [39].

Recently, machine learning (ML) has been explored to speed-up TE in large-scale networks. By using ML algorithms such as graph neural network (GNN) or reinforcement learning (RL), networks can automatically learn and adapt to traffic patterns, predict congestion, and optimize routing in real-time. This results in improved network performance, reduced latency, and better resource utilization [22], [31], [29], [41], making ML a promising tool for modern TE.

However, despite early success, current learning-based TE algorithms have several inherent limitations, which significantly hinder their application in real-world networks. First, existing algorithms are trained on the same network topology as testing or inference, and can adapt to at best minor topology changes such as individual link or node failures [30], [39]. This leads to inferior generalizability of the trained models, making them perform poorly on unseen topologies (such as when deployed in a new network) or in face of major topology changes (such as regional failures). The most generalizable learning-based TE solution to-date can adapt to up to 20% topology changes, such as local link failures or congestion. They also do not generalize to traffic patterns substantially different from the training data, such as during periods with abnormal traffic. If the network conditions change majorly after training completes, the models must be completely retrained, causing significant time and computational overhead.

Second, many algorithms require extensive training time and computation power. For instance, a state-of-the-art solution

TEAL [39] needs to be trained on latest GPU for more than a week for a network with over 1700 nodes, and another state-of-the-art solution HARP [3] encounters prohibitive memory usage when scaling to networks with over 1000 nodes. This makes it very difficult to (re-)train models for different network scenarios and conditions. Furthermore, some models do not always respect TE constraints such as link capacities and may cause excessive violations in some situations, in which case computationally expensive classical algorithms, such as ADMM—the alternating direction method of multipliers, have to be used to ensure feasibility and avoid causing excessive congestion [39].

To address these challenges, we propose **TELG**EN, a novel end-to-end learning-based TE algorithm for large-scale networks. TELGEN is designed to efficiently solve TE problems in networks with diverse sizes and shapes, traffic patterns and conditions without or with minimal re-training. To achieve both optimality and generalizability, TELGEN employs a *flexible GNN architecture* that is agnostic to the topology or traffic demands, and is trained with (*step-by-step supervised learning*) to mimic the most powerful classical TE algorithms with high efficiency and optimality. Specifically, by casting TE problems as LPs, TELGEN learns the detailed steps that a classical TE algorithm (such as the interior-point method or IPM) takes to solve smaller-scale TE problems till optimality, and then generalizes the learned algorithm to larger networks and problem sizes utilizing the invariance properties of GNNs. Employing strong supervision from the classical algorithm significantly improves convergence and reduces training overhead in terms of the amount of data and computation needed.

We trained and evaluated TELGEN on a wide range of randomly generated and real-world network topologies. Experiments showed that TELGEN could achieve close-to-optimal TE (with $< 3\%$ optimality gap while ensuring feasibility), was up to 7 times faster than a state-of-the-art IPM solver, and achieved up to 2 orders of magnitude reduction in training time per epoch and prediction time over TEAL and 4 orders of magnitude reduction over HARP on large network topologies. Further, TELGEN maintained negligible optimality gap even when the test networks were 2–20 \times larger than the largest network in training, or when demand patterns varied largely between training and testing, demonstrating superior generalizability in face of diverse network scenarios and conditions.

To summarize, our main contributions are as follows:

- We propose a flexible GNN architecture for modeling and learning efficient TE algorithms that is agnostic to network topology, size, condition and traffic demands.
- We propose a general supervised learning approach to efficiently learn close-to-optimal and generalizable GNN-based algorithms for solving large-scale TE problems, by mimicking classical TE algorithm on smaller instances during training, and testing on larger, diverse networks.
- We conducted extensive simulations on randomly generated and real network topologies with up to 5000 nodes. Experiments showed the superior optimality, training and inference efficiency, and generalizability of TELGEN w.r.t. state-of-the-art solver and learning-based solutions.

In the following, Sec. II discusses related works. Sec. III describes the system model and problem formulation. Sec. IV describes the proposed GNN architecture and the training algorithm for solving large-scale TE problems. Sec. V shows evaluation results. Sec. VI concludes this paper.

II. BACKGROUND AND RELATED WORK

A. Traffic Engineering

The primary goal of TE is to direct traffic within a data network to meet traffic demands by optimizing a chosen performance metric [26]. State-of-the-art TE solutions rely on formulating it as an LP or a convex program, which can be solved by commercial solvers using standard optimization algorithms (such as IPM, simplex method or primal-dual methods). However, the swift expansion and addition of new data centers or the emergence of new networks such as large-scale LEO satellite networks have made the TE optimization decision making process exceedingly slow and impractical at larger scales. Nowadays, it takes commercial solvers several hours to allocate traffic on WANs comprising thousands of nodes [39]. As a result, WAN operators are urgently looking for ways to expedite TE optimization to match the rapid growth of their networks. Methods have been proposed to parallelize LP solvers, which can only achieve a coarse-level parallelization over CPUs and at best a moderate speed-up and no asymptotical improvement [2], [27]. Approximation algorithms such as Fleischer’s algorithm [13] have also been a solution to speed up TE, which nevertheless compromises optimality and can lead to many iterations to converge.

B. Machine Learning for Traffic Engineering

Methods have emerged to utilize ML to address the scalability issue in TE, with some promising initial results on significantly accelerating TE optimization [4], [24], [33], [35]. By training on historical or randomly generated data, ML models can make accurate predictions that enhance the efficiency of network management. Early approaches began with using Convolutional Neural Networks (CNNs) to efficiently handle spatial dependencies in network data [25], focuses on predicting traffic matrices as inputs to traditional TE algorithms. Subsequent works have explored deep RL to solve various TE problems including TE automation, delay minimization, power-awareness and dynamic changes of traffic demands [22], [29], [31], [41]. While promising, simple (deep) RL algorithms are difficult to encode or learn detailed network information such as topology and capacity constraints, and can lead to unstable performance or frequent capacity violations in practice. Some works have used GNNs for network performance modeling or prediction which could assist TE [11], [12], but do not directly address the efficiency and scalability bottleneck of classical TE solvers.

In TEAL [39], the authors combined multi-agent RL (MARL) with a GNN-based feature extractor to learn network-specific information (such as topology and flows), and applied classical ADMM to ensure feasibility. The GNN-MARL model was trained with historical or randomly generated demands on the target network, and performed reasonably well *on the same network* with different but similar demands.

However, TEAL can only be applied to the exact same set of source-destination (SD) pairs on the same network as training, and have to be re-trained from scratch even when a new node is added or an existing node is removed, significantly limiting its generalizability. It also suffers from significant training time and overhead due to the use of RL, and cannot satisfy link capacity constraints without substantial help from ADMM.

Compared to RL-based solutions, another approach is to directly learn a mapping from problem inputs (or historical demands) to the TE solution, such as DOTE [30] and FIGRET [23]. These algorithms directly learn and encode the network topology into the neural model parameters, and hence cannot generalize to topologies beyond the training network. Recently, a *transferable* neural model called HARP was proposed for minimizing the maximum link utilization (MLU) in TE [3], which can adapt to topology variation with up to 20% difference in links. HARP is specially designed to minimize MLU and cannot be adapted to other TE objectives without modifying the model architecture. The goal of HARP's transferable design is to consider continuous topology changes such as local link/node failures during TE operations, and it does not tackle the issue of generalizing predictions to networks significantly different from or larger than training. Compared to HARP, our proposed TELGEN can generalize to networks with up to $20\times$ more nodes than those in training, owing to its principled design around *generalizability*.

C. Graph Neural Network

GNNs [37] have emerged as a powerful framework for machine learning on graph-structured data. Let a graph be represented as $G = (V, E)$, where V is the node set and E is the edge set of the graph. The neighbor node set of a node v is defined as $N(v) = \{u \in V \mid (v, u) \in E\}$. Define the adjacency matrix $A^{n \times n}$ with $A_{ij} = 1$ if $e_{(i,j)} \in E$, and 0 otherwise, with $n = |V|$. Let h_v be the node attribute for $v \in V$. A GNN model consists of a fixed number of GNN layers, denoted by K , and let a node's attribute after layer k be h_v^k . In each layer k , a message passing function denoted as $\text{msg}^k(\cdot)$ is applied to pass and aggregate the node attributes of all neighbors of each node v , and an aggregation function denoted as $\text{aggr}^k(\cdot)$ is then applied to aggregate the aggregated neighbor messages with the node's own attribute h_v^{k-1} , outputting the updated node attribute h_v^k . A GNN layer can thus be represented as:

$$h_v^k = \text{aggr}^k(h_v^{k-1}, \text{msg}^k(\{h_u^{k-1} \mid u \in N(v)\})). \quad (1)$$

To make a prediction, a readout function $r(\cdot)$ is further applied to node attributes after layer K to predict the target node, link or graph-level labels. In a GNN, the functions msg^k , aggr^k and r are modeled by parameterized neural networks (such as multi-layer perceptrons or MLPs), whose parameters are trained with training data guided by a loss function.

GNNs are increasingly utilized both as direct solvers and to augment existing solvers [5]. In [19], a learning-based method for solving the Travelling Salesman Problem has been proposed via deep graph convolutional networks. An imitation learning framework of branch-and-bound has been proposed by [40] to parameterize the state of the branch-and-bound search tree for heterogeneous Mixed-Integer Linear

Programming problems. Likewise, [21] tackled combinatorial problems that can be reduced to the Maximum Independent Set, Minimum Vertex Cover, Maximal Clique and Satisfiability using GNN models. Follow-up research such as [5] studied solvers augmented by RL and observed that the GNN component is crucial for achieving competitive solution quality. Despite their general popularity, GNNs are used in most existing works to augment other solvers, rather than as end-to-end solvers themselves.

III. SYSTEM MODEL AND PROBLEM FORMULATION

The goal of TE is to allocate network resources among clients and optimize for network performance, such as maximizing throughput, minimizing latency, or minimizing maximum link utilization (MLU). The widely used TE formulation involves splitting traffic demands between source-destination (SD) pairs along multiple paths. This involves determining the best routes for data packets to travel and balancing the load across various network paths to avoid congestion and ensure efficient utilization of bandwidth. Without loss of generality, we assume the objective of the network operator is to maximize the overall network throughput when meeting the demands of network SD pairs, subject to the link capacities.

A. Network Model

Network. The network is denoted as a directed graph $\mathcal{G} = (N, L, C)$, where N is the set of nodes, L is the set of links between nodes, and $C : L \rightarrow \mathbf{R}^+$ denotes the capacity of each link; \mathbf{R}^+ is the non-negative real number set. There are in total $|N|$ nodes and $|L|$ links in \mathcal{G} .

Client demands. We consider a set of SD pairs, $(s_i, t_i, d_i) \in D$, where s_i and t_i are the source and destination nodes of SD pair i respectively, and $d_i \in \mathbf{R}^+$ is the traffic demand; we use i and (s_i, t_i, d_i) interchangeably when referring to an SD pair. We assume the demands are either given as input, or predicted by a traffic prediction model independent from the TE system.

Predefined network paths. The set of network paths for an SD pair i is denoted by P_i . Without loss of generality, we assume no two SD pairs have the same source and destination (s_i, t_i) , and define $P = \bigcup_i P_i$. We write $n \in p$ and $l \in p$ to denote a node and a link that a path p passes through, respectively. Following most existing TE solutions [23], [30], [39], we assume the set of paths for each SD pair is given as input to the TE system. It can, for instance, be calculated by Yen's k -shortest path algorithm [9] between each SD pair.

B. TE Optimization Problem Formulation

Traffic Splitting. The basic TE problem has decision variables, defined as *traffic splitting ratios* \mathcal{R} , which denote allocated fractions of each SD pair's demand to possible paths of the SD pair. We define $\mathcal{R}(p)$ as the fraction of the demand d_i that is allocated to path $p \in P_i$. The total traffic split ratio of an SD pair cannot exceed 100%. We thus represent the variables as a mapping $\mathcal{R} : P \rightarrow [0, 1]$, and enforce this constraint in the formulation as described below.

Objective. The basic goal of TE optimization is to maximize network flow for all demands. This leads to the objective function as: maximize $f_0(\mathcal{R}) \triangleq \sum_{i \in D} d_i \sum_{p \in P_i} \mathcal{R}(p)$. We use this throughput maximization objective as the primary example in our description and evaluation, although our designed solution should be adaptable to other linear objectives (such as minimizing MLU or routing cost), and possibly convex non-linear objectives as well (such as fairness).

Constraints. The problem has two sets of constraints. First, the total allocated traffic for each SD pair cannot exceed its demand, and hence $\sum_{p \in P_i} \mathcal{R}(p) \leq 1$ for every $i \in D$. Second, the traffic allocated on a link cannot exceed its capacity, and hence we have $\sum_{i \in D} d_i \sum_{p \in P_i: l \in p} \mathcal{R}(p) \leq C(l)$ for $\forall l \in L$.

TE Optimization. We formulate TE optimization as:

$$\begin{aligned} & \text{maximize} && f_0(\mathcal{R}) \triangleq \sum_{i \in D} d_i \sum_{p \in P_i} \mathcal{R}(p) \\ & \text{subject to} && \sum_{p \in P_i} \mathcal{R}(p) \leq 1, \quad \forall i \in D; \\ & && \sum_{i \in D} d_i \sum_{p \in P_i: l \in p} \mathcal{R}(p) \leq C(l), \quad \forall l \in L; \\ & && \mathcal{R}(p) \geq 0, \quad \forall p \in P. \end{aligned} \quad (2)$$

For simplicity, we define constraint functions $f_i^D(\mathcal{R}) \triangleq \sum_{p \in P_i} \mathcal{R}(p) - 1$, and $f_l^L(\mathcal{R}) \triangleq \sum_{i \in D} d_i \sum_{p \in P_i: l \in p} \mathcal{R}(p) - C(l)$. We want to design an algorithm that solves (6) to its optimality, ensures feasibility of the solution, and can do so efficiently on very large network scenarios (with thousands of nodes) even on those not observed in the training process.

IV. TELGEN: A LEARNING-BASED TE FRAMEWORK

A. Motivation and Overview

Compared to prior work, our first-class goal is to learn *generalizable* neural models that can efficiently solve Program (6) on different network conditions, including different topologies, link capacities and demand distributions. In principle, one can achieve these goals by developing models that can work with different sets of inputs, and then training these models with diverse training data to achieve generalizability. Unfortunately, most ML models (e.g. MLP, CNN or Transformer) do not have such flexibility due to their fixed input sizes or shapes, rendering solutions such as DOTE [30] intrinsically non-generalizable. Compared to other models, GNNs present a natural architecture that is invariant to permutation of input data, which means the output will not change when given such inputs, making them suitable to train generalizable models as demonstrated on various graph-alike data [14]. This motivates us to propose a general TE framework using GNNs.

To apply GNNs for TE, a naive idea is to use a GNN to directly model the network structure. This has been adopted in network performance modeling, e.g., utilizing GNNs to predict network queueing delays [12]. However, it is not trivial to extend this idea to modeling the correlations among routing paths, traffic allocation and link capacities, as each path may consist of multiple links; it is also unclear how to represent a global objective function such as the total throughput or the maximum link utilization. Our solution thus develops a

new GNN architecture, which not only represents the network topology, but also the correct correlations among paths, links and network-wide objectives in one graph. This is achieved by transforming the LP formulation in Program (6) into a graph, thus preserving all the information in the TE formulation.

To train a neural TE model, existing works rely on the TE objective and/or constraints as the only supervising signal for training, by defining them directly as the loss function or the reward function in RL. However, this can lead to extremely long training epochs, and the trained model can usually reach a local optimum which is not necessarily a global optimum. To address this issue, we draw inspiration from recent advances in ML on *algorithmic alignment* [38], and develop GNN models that are directly *aligned* to classical optimization algorithms (such as IPM). These models can then be trained directly with **strong supervision** from the intermediate steps generated by the classical algorithms, both achieving efficient training and ensuring convergence to the global optimal solutions that are output by these algorithms. Since these classical algorithms are *agnostic* to the network structure or input distributions—they are designed to solve any TE instance to optimality—the trained models will naturally learn such behaviors during training, thereby achieving inherent generalizability.

Next, we explain detailed design of our solution, and use IPM as the classical algorithm for supervision. For completeness, we start with a brief introduction to the state-of-the-art IPM algorithm, and then describe our solution in details.

B. IPM Preliminaries

IPM [28] is an efficient algorithm for optimally solving LPs and convex programs, and is widely adopted in commercial solvers [16], [17], [34]. Consider a standard LP formulated as $\max_{\mathbf{x}} \{ \mathbf{c}^T \mathbf{x} \mid \mathbf{A} \mathbf{x} \leq \mathbf{b}, \mathbf{x} \geq 0 \}$ with coefficient matrix \mathbf{A} and constant vectors \mathbf{b}, \mathbf{c} . A standard IPM [32] is shown in Algorithm 1. It starts from an initial strictly feasible solution \mathbf{x}_0 , and then traverse the interior of the feasible region to find the optimal solution. At each iteration, a search direction is determined, and a step size is calculated to ensure the new solution remains feasible while reducing a barrier function parameter μ . The barrier parameter μ guides the solution towards the optimal point by penalizing infeasibility. The iterations continue until μ is sufficiently small, at which point the current solution \mathbf{x}_k is considered approximately optimal.

The primary bottleneck of IPM is the complexity of solving large linear systems of equations (the Newton’s step in Line 5) at each iteration. The fastest linear solver runs in almost cubic time, significantly limiting scalability of IPM beyond modest problem sizes. Meanwhile, due to its use of the Newton’s step, IPM can converge to optimality in almost a constant number of iterations in most practical settings, typically less than 5-30 iterations regardless of problem size [15]. This makes IPM a particularly good candidate to be mimicked and sped-up by ML—speeding-up the Newton’s step will yield good asymptotic improvement, while the small number of iterations is ideal for algorithmic alignment, as we discuss in Sec. IV-D.

Algorithm 1 IPM for Linear Programming

Require: Problem data \mathbf{A} , \mathbf{b} , \mathbf{c} ; initial barrier parameter $\mu_0 > 0$; error tolerance $\epsilon > 0$; discount factor $\tau \in (0, 1)$

- 1: Choose initial feasible solution \mathbf{x}_0 such that $\mathbf{Ax}_0 < \mathbf{b}$ and $\mathbf{x}_0 > 0$
- 2: Set the initial barrier parameter $\mu \leftarrow \mu_0$, and $k \leftarrow 0$
- 3: **while** $\mu > \epsilon$ **do**
- 4: $k \leftarrow k + 1$
- 5: Compute Newton direction $\Delta \mathbf{x}_k$ on barrier problem $\max_{\mathbf{x}} \{ \mathbf{c}^\top \mathbf{x} - \mu (\mathbf{1}^\top \log(\mathbf{b} - \mathbf{Ax}) + \mathbf{1}^\top \log(\mathbf{x})) \}$
- 6: Perform a line search to determine step size α_k that ensures that $\mathbf{x}_k = \mathbf{x}_{k-1} + \alpha_k \Delta \mathbf{x}_k$ remains feasible
- 7: Update the solution $\mathbf{x}_k \leftarrow \mathbf{x}_{k-1} + \alpha_k \Delta \mathbf{x}_k$
- 8: Reduce the barrier parameter $\mu \leftarrow \tau \mu$
- 9: **end while**
- 10: **return** approximately optimal solution \mathbf{x}_k .

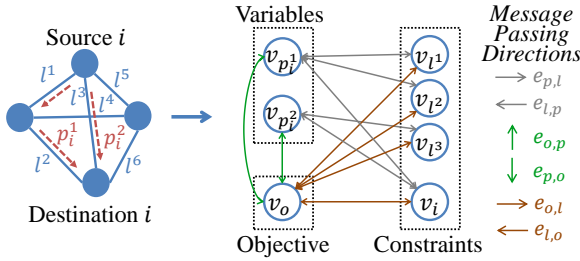


Fig. 1: Graph representation of TE instance with one SD pair and two paths. Each vertex denotes a variable, a constraint, or the objective. Directed edges denote their correlations in the LP formulation. GNN message passing will be carried out along the edges in six directions, as detailed in Sec. IV-E.

C. Representing TE as a Graph

To speed-up TE, our first step is to represent the TE problem as a neural model that can be trained. As we motivated in Sec. IV-A, a simple GNN defined over the network topology graph itself cannot effectively embed information such as decision variables (path traffic split ratios), constraints and the objective. To this end, we develop a new GNN architecture, where the graph is not defined on the network but on all the entities (variables, constraints and objective) and their correlations presented in the LP formulation in Program (6).

Consider the GNN graph $G = (V, E)$ where V is defined by four sets of vertices: set V^p denotes path vertices with $v_p \in V^p$ for each $p \in P$; set V^d denotes SD pair vertices with $v_i \in V^d$ for each SD pair $i \in D$; set V^l denotes link vertices with $v_l \in V^l$ for each link l ; and a single vertex v_o denotes the network-wide objective function in Program (6). Each vertex in V^p represents a *traffic splitting variable* $\mathcal{R}(p)$, each vertex in V^d represents a *demand constraint*, and each vertex in V^l represents a *capacity constraint*.

Edge set E contains undirected edges that model correlations among path variables, link constraints, and the objective function. The set E^{pd} contains edges $e_{p,i}$ that each models the correlation between path p and SD pair i 's demands, for $p_i \in P_i$. The set E^{pl} contains edges $e_{p,l}$ that each models the

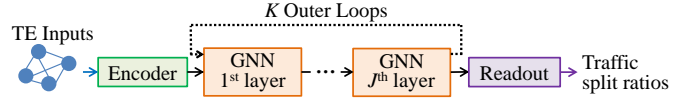


Fig. 2: Double-looped GNN architecture: K outer loops simulating IPM iterations, and J inner layers to learn an IPM step.

correlation between path p and link l , if $l \in p$. The set E^{po} contains edges $e_{p,o}$ that each models the correlation between path p and objective o . The set E^{do} contains edges $e_{i,o}$ that each models the correlation between SD pair i and objective o . The set E^{lo} contains edges $e_{l,o}$ that each models the correlation between link l and objective o . Intuitively, edges E^{pd} represent each path's traffic split ratio contribute to the demand of its SD pair, and edges E^{pl} represent how allocations on paths through the same link are bounded by the link capacity. Edges E^{po} represent how each path's traffic split ratio contributes to maximizing the total throughput (the objective). While edges E^{do} and E^{lo} may seem disconnected from Program (6)—there is no direct relationship between the constraints and the objective—they can in fact be interpreted as the implicit correlations between the *dual variables* corresponding to the constraints, and the *dual objective* which is equal to the primal objective by strong duality of LP. Each edge is labeled with the corresponding coefficient in Program (6). For instance, edge $e_{p,i} \in E^{pd}$ for path p would have weight 1 as the coefficient of variable $\mathcal{R}(p)$ in the demand constraint, and edge $e_{p,l} \in E^{pl}$ for $p \in P_i$ would have weight d_i as in the capacity constraint.

Fig. 1 shows the GNN graph representation for a network with four nodes and six links. Given SD pair i , there are two possible paths p_i^1, p_i^2 (red dash lines), which are represented by the variable vertices: $v_{p_i^1}$ and $v_{p_i^2}$. The capacity constraints for the three links l^1, l^2, l^3 are represented by constraint vertices v_{l^1}, v_{l^2} and v_{l^3} . v_i represents the single demand constraint, and v_o represents the objective. The gray edges $e_{p,i}$ and $e_{p,l}$ models the relations between the variable vertices and the constraint vertices. The green edges $e_{p,o}$ models the relations between the variable vertices and the objective vertex. The brown edges $e_{i,o}$ and $e_{l,o}$ models the relations between the constraint vertices and the objective vertex. Here, we represent this TE as a GNN.

The key principle behind the above construction, as also hinted by existing work [6], [20], [32], [39], is to fully represent all information within the LP formulation in the same model. Correlations among variables, constraints and the objective are fully captured by the edges, while all problem data are encoded as weights on the edges. The model can further easily generalize to adding, removing or permuting of variables and constraints. Next, we further talk about how the GNN model can be aligned to the IPM algorithm, and how it can also be trained under strong supervision by IPM.

D. Algorithmic Alignment and Strongly Supervised Training

While existing work such as [32], [39] utilized similar GNN structures as above, they trained their model to directly optimize for the objective function, regularized by constraint penalty. This may however lead to difficulty in convergence, or converging to local optima that are far from global optimality.

Motivated by the algorithmic alignment literature in ML [6], [38], we are inspired to better align our GNN model with the IPM algorithm to achieve strong performance and generalizability. Since an IPM iteration basically takes a Newton's step from the previous iteration's solution, starting from an initial feasible solution, we want the GNN model to learn the same behavior. To this end, we define a **double-looped** GNN architecture, which consists of K outer GNN layers, and J inner GNN layers in each outer layer, as in Fig. 2. Each outer layer corresponds to an IPM iteration, and seeks to mimic one Newton's update on the previous layer's solution (represented by vertex attributes after previous layer). The number of outer layers, K , should correspond to the number of iterations that IPM takes to converge, which is usually a constant that can be easily estimated [32].

Because each outer layer corresponds to the same operation (Newton's step) that is applied on a different input (previous iteration's solution), the message passing function msg^k and the aggregation functions aggr^k in all outer GNN layers should share the same neural network parameters. Furthermore, since the IPM generates a feasible solution in every iteration, each GNN outer layer's output can be supervised by a loss function defined between the GNN's output solution (by applying the readout function r) and the IPM's updated solution. This **strong supervision** of each GNN layer's output can greatly improve the model's ability to learn not just the optimal solutions in the training dataset, but also the *trajectories of convergence to optimality* by IPM. This is crucial for the neural model to learn the generalizability of the optimal algorithm—to converge to optimality given *any* problem instance.

One concern in the above architecture is whether one (outer) GNN layer can well approximate the Newton's step, which is a fairly complex operation that warrants a nearly cubic complexity. To this end, we further expand each outer layer to consist of J inner GNN layers. Intuitively, these layers are to learn the intermediate steps in solving the Newton's system, plus applying the system's solution to the variables' update. Since these steps do not correspond to feasible solutions to the original problem, the inner GNN layers are unsupervised. In practice, we find that $J = 2$ inner layers are already sufficient for even the largest networks that we evaluate.

E. Model Design and Training Procedures

With the above discussions, we now describe the GNN model and training procedures for solving large-scale TE problems with generalizability as depicted in Fig. 2. The GNN model consists of J sets of message passing and aggregation functions msg_j and aggr_j corresponding to the J inner layers, and one readout function r . Each msg_j contains six distinct functions: $\text{msg}_j^{\text{p-dl}}$, $\text{msg}_j^{\text{dl-p}}$, $\text{msg}_j^{\text{p-o}}$, $\text{msg}_j^{\text{o-p}}$, $\text{msg}_j^{\text{dl-o}}$, and $\text{msg}_j^{\text{o-dl}}$. Each aggr_j contains three functions: aggr_j^{p} , $\text{aggr}_j^{\text{dl}}$, and aggr_j^{o} . For $\alpha, \beta \in \{\text{p}, \text{dl}, \text{o}\}$, the functions $\text{msg}_j^{\alpha-\beta}$ and aggr_j^{β} are used to update the vertex attributes of V^β based on the attributes of V^α , where p denotes path vertices, dl denotes demand and link vertices, and o denotes the objective vertex. We cluster demand and link vertices together since all constraints can be normalized to have the same right-hand-side, *i.e.*, let $\mathbf{b} = 1$ in

the LP formulation. All functions are shared across all outer layers, and the model can have a variable number of outer layers depending on the input instance.

The initial vertex attributes are denoted by $h_p^{0,0}$, $h_{\text{dl}}^{0,0}$ and $h_o^{0,0}$ respectively. These can be either fixed values, or problem-specific such as the mean and variance of each row/column. Each GNN layer (outer k inner j) then updates vertex attributes based on the update rules below:

$$\begin{aligned} h_{\text{dl}}^{k,j} &= \text{aggr}_j^{\text{dl}} \left(h_{\text{dl}}^{k,j-1}, \text{msg}_j^{\text{p-dl}}(\{h_p^{k,j-1} | e_{p,i} \in E^{\text{pd}}, e_{p,l} \in E^{\text{pl}}\}), \right. \\ &\quad \left. \text{msg}_j^{\text{o-dl}}(\{h_o^{k,j-1} | e_{i,o} \in E^{\text{do}}, e_{l,o} \in E^{\text{lo}}\}) \right); \\ h_o^{k,j} &= \text{aggr}_j^{\text{o}} \left(h_o^{k,j-1}, \text{msg}_j^{\text{dl-o}}(\{h_{\text{dl}}^{k,j} | e_{i,o} \in E^{\text{do}}, e_{l,o} \in E^{\text{lo}}\}), \right. \\ &\quad \left. \text{msg}_j^{\text{p-o}}(\{h_p^{k,j-1} | e_{p,o} \in E^{\text{po}}\}) \right); \\ h_p^{k,j} &= \text{aggr}_j^{\text{p}} \left(h_p^{k,j-1}, \text{msg}_j^{\text{dl-p}}(\{h_{\text{dl}}^{k,j} | e_{p,i} \in E^{\text{pd}}, e_{p,l} \in E^{\text{pl}}\}), \right. \\ &\quad \left. \text{msg}_j^{\text{o-p}}(\{h_o^{k,j} | e_{p,o} \in E^{\text{po}}\}) \right). \end{aligned}$$

To train the GNN model, the training dataset (of size M_{tr}) contains real or synthetic TE instances, each defined by a network topology and a set of SD pairs with demands. An IPM algorithm is used to first solve each training instance to optimality, and the intermediate solutions are saved as part of the training dataset to supervise training. Let $\widehat{\mathcal{R}}_k^{(\tau)}$ be the k -th IPM iteration's output solution when processing training instance τ , and $\mathcal{R}_k^{(\tau)}$ be the solution output by applying the readout function r to each variable vertex's attribute in V^{p} . The training loss function consists of three loss components:

(1) The *variable loss* is defined as:

$$\mathcal{L}_{\text{p}} = \frac{1}{M_{\text{tr}}} \sum_{\tau=1}^{M_{\text{tr}}} \sum_{k=1}^{K_{\tau}} \xi^{K_{\tau}-k} \cdot \left| \mathcal{R}_k^{(\tau)} - \widehat{\mathcal{R}}_k^{(\tau)} \right|_2^2,$$

where K_{τ} is the number of IPM iterations (and hence number of outer loops) for instance τ , and ξ is a discount factor for each iteration to prioritize convergence in the later iterations.

(2) The *constraint loss* is defined as:

$$\begin{aligned} \mathcal{L}_{\text{dl}} &= \frac{1}{M_{\text{tr}}} \sum_{\tau=1}^{M_{\text{tr}}} \sum_{k=1}^{K_{\tau}} \xi^{K_{\tau}-k} \cdot \left(\sum_{i \in D^{(\tau)}} \text{ReLU} \left(f_i^D(\mathcal{R}_k^{(\tau)}) \right) \right. \\ &\quad \left. + \sum_{l \in L^{(\tau)}} \frac{\text{ReLU} \left(f_l^L(\mathcal{R}_k^{(\tau)}) \right)}{C(l)} \right), \end{aligned}$$

where ReLU is a rectified linear unit, and $D^{(\tau)}$ and $L^{(\tau)}$ are the corresponding demand set and link set in problem instance τ . The constraint loss is defined as the constraint violation of solution generated in every GNN outer loop, normalized by the right-hand-side constant of each constraint. It penalizes the output solution of each outer loop to ensure feasibility of the solution update trajectory, in line with the original IPM.

(3) Finally, the *objective loss* is defined as:

$$\mathcal{L}_{\text{o}} = \frac{1}{M_{\text{tr}}} \sum_{\tau=1}^{M_{\text{tr}}} \sum_{k=1}^{K_{\tau}} \xi^{K_{\tau}-k} \cdot \left| f_0(\mathcal{R}_k^{(\tau)}) - f_0(\widehat{\mathcal{R}}_k^{(\tau)}) \right|_2^2.$$

The objective loss penalizes when the generated solutions deviate too much from the IPM's updates in each iteration.

TABLE I: Statistics of network topology sizes in each training and test dataset

Dataset	Erdős-Rényi Training	Waxman Training	B4 Training	ASN Training
# of nodes	20, 30, ..., 100	200, 300, ..., 800	12	217, 237
# of edges	$O(10^2)$, ..., $O(7.9 \times 10^3)$	$O(6 \times 10^2)$, ..., $O(4 \times 10^3)$	38	$O(6 \times 10^2)$
Dataset	Erdős-Rényi Test	Waxman Test	B4 Test	ASN Test
# of nodes	200, 500, 1000, 2000	2000, 3000, 4000, 5000	12	553, 1739
# of edges	$O(2.8 \times 10^4)$, ..., $O(3.6 \times 10^6)$	$O(1.1 \times 10^4)$, ..., $O(2.1 \times 10^4)$	38	$O(1.6 \times 10^3)$, $O(9 \times 10^3)$

With the above, the final training loss is defined as

$$\mathcal{L} = \rho_1 \mathcal{L}_p + \rho_2 \mathcal{L}_{dl} + \rho_3 \mathcal{L}_o. \quad (3)$$

V. PERFORMANCE EVALUATION

A. Datasets

To thoroughly evaluate the performance and generalizability of our algorithm, we generated four datasets for training and testing: two with randomly generated topologies, and two with practical, real-world topologies. Each dataset has a training set and a test set. Their statistics are summarized in Table I.

Erdős-Rényi (ER) Dataset: We generated random topologies based on the Erdős-Rényi model [10]. For *training set*, we generated networks with $\{20, 30, \dots, 100\}$ nodes, each with a connection probability of $\{0.3, 0.4, \dots, 0.8\}$. This resulted in $9 \times 6 = 54$ topology configurations, and we generated 200 instances for each configuration. For each instance, 10 random SD pairs were selected. The link capacities and SD pair demands were both randomly generated in $[1000, 5000]$; the same default range applies to all other datasets below. For *test set*, we generated significantly larger networks with $\{200, 500, 1000, 2000\}$ nodes respectively, with connection probability in $\{0.7, 0.8, 0.9\}$. Each of the 12 test configuration had 300 instances with the same number of SD pairs and range for demands and capacities; we denote these 12 test sets as $ER_{n,q}^{\text{test}}$, where n is the node number, q is the connection probability. The largest topology in training set had almost 8×10^3 links, and the largest topology in test set had 3.6×10^6 links, two to three orders of magnitude larger than training.

Waxman (WA) Dataset: We generated random networks based on Waxman’s model [36]. For *training set*, we generated networks with $\{200, 300, \dots, 800\}$ nodes with default connection parameters $\alpha = 0.1$ and $\beta = \{0.2, 0.18, \dots, 0.08\}$ ¹. Each configuration had 800 instances, and each instance had 20 random SD pairs. For *test set*, we generated large networks that had $\{2000, 3000, 4000, 5000\}$ nodes, with default connection parameters $\alpha = 0.1$ and $\beta = \{0.03, 0.02, 0.015, 0.01\}$ respectively, each with 500 instances. We set these parameters so that the generated networks had similar node/link ratios as the real-world one (ASN). We denote the test sets as WA_n^{test} for node number n . The largest topology in training set had 4×10^3 links, and the largest topology in test set had 2×10^4 links, five times larger than training.

B4 and ASN Datasets²: Two real-world network topologies were used for evaluation which were also used in [39]: Google’s cloud-WAN topology B4 [18], and Microsoft’s AS-level Internet topology denoted as ASN [1]. B4 is a small topology with 12 nodes and 38 links. Thus we trained and tested on the same topology, with 200 and 50 training and test instances respectively. ASN is a large topology with 1739 nodes and 8558 links. For ASN, we chose two randomly sampled subgraphs as training set, with 217 and 237 nodes and each around 600 links respectively; 2000 instances were generated for each subgraph. We tested on the largest connected component of ASN *after pruning all nodes in the training set*, with 553 nodes denoted as ASN_{553}^{test} and around 1600 links, as well as the full ASN topology denoted as ASN_{1739}^{test} ; each had 500 test instances. The largest test instance in ASN had more than $10 \times$ links than the largest training instance.

B. Implementation and Evaluation Setup

Comparison Algorithms: We compared TELGEN to two state-of-the-art learning-based TE solutions, TEAL [39] and HARP [3], as well as the optimal SciPy IPM solver as the baseline. Below, we describe their implementation details³.

1) *TELGEN*: We extended the GNN codebase in [7] to implement TELGEN. The GNN model consisted of MLP encoders each to encode the initial attributes of one set of vertices in $\{V^p, V^{d \cup V^l}, \{v_o\}\}$, a series of graph convolutional (GCN) layers for message passing among vertices, and an MLP readout function to generate the TE solution from each path vertex’s attribute in V^p ; a ReLU layer was applied after readout to ensure non-negativity of the TE solution.

All encoders were two-layer MLPs with hidden dimensions 180 and 360. We used $J = 2$ GCN layers for the inner loop. For ER and B4 datasets, we used 8 outer layers; for Waxman and ASN, we used 16 outer layers. The hidden dimensions of the readout two-layer MLP were 360 and 720. The model was trained independently for 150 epochs on ER and WA datasets, and 50 epochs on the B4 and ASN datasets.

2) *TEAL* [39]: We used the open-source implementation of TEAL which solves TE with the same objective as TELGEN—maximizing the total flow. For fair comparison, we translated datasets generated for TELGEN into the same format as TEAL’s input, and compared their performance on the same

²These are the smallest and largest topologies evaluated in [39] respectively, though we train and test on different SD pairs and demands than original paper.

³Our implementation code is available at https://github.ncsu.edu/NCSU-Yu-Research-Group/TE_TELGEN/

¹Here the α, β are Waxman parameters [36], not those used in Sec. IV-E.

datasets. As a remark, TEAL is designed in a way such that testing must be on the same topology and SD pairs as training.

3) *HARP* [3]: We used the open-source implementation of HARP, and translated our datasets into the input format of HARP. Note that HARP’s model architecture is specifically designed to minimize the MLU, and cannot generalize to other objectives such as the total flow maximization as in TEAL or TELGEN. To make sure the solutions are comparable under the same objective, we scale HARP’s traffic split ratios such that they fully respect the link capacities (*i.e.*, $MLU = 1$).

One issue of HARP is that it has a large memory footprint on large topologies, and even the latest hardware platform available to us (as below) could not execute HARP on the largest topology—the full ASN. To make a fair comparison, we trained and tested all three algorithms above on B4, and randomly sampled smaller subnetworks of ASN.

4) *SciPy* [8]: The `scipy.optimize.linprog` routine was used to optimally solve the LP with IPM, and the per-iteration solution was recorded to supervise training of TELGEN.

Hardware platform: All the algorithms were implemented and evaluated on a desktop server with Intel Xeon Gold 5317 CPU (3.0GHz, 48 cores), 256GB RAM and Nvidia A100 GPU (40GB). All experiments were run with 3 random seeds and averages are shown below.

C. Evaluation Metrics

We consider five metrics for comparison among algorithms. Consider a test set with M_{ts} instances. The *objective gap* (**OGap**) is defined as the mean absolute difference between the objective value of the final algorithm output solution $\widehat{\mathcal{R}}^{(\tau)}$ and the optimal solution $\widehat{\mathcal{R}}^{(\tau)}$ (output by the IPM solver) for test instant τ , normalized by the optimal value:

$$\gamma_{obj} \triangleq \frac{1}{M_{ts}} \sum_{\tau=1}^{M_{ts}} \left| \frac{f_0(\mathcal{R}^{(\tau)}) - f_0(\widehat{\mathcal{R}}^{(\tau)})}{f_0(\widehat{\mathcal{R}}^{(\tau)})} \right|. \quad (4)$$

The *constraint gap* (**CGap**) is the mean absolute constraint violation of the final algorithm output solution:

$$\gamma_{con} = \frac{1}{M_{ts}} \sum_{\tau=1}^{M_{ts}} \left(\sum_{i \in D^{(\tau)}} \text{ReLU}(f_i^D(\mathcal{R}^{(\tau)})) + \sum_{l \in L^{(\tau)}} \frac{\text{ReLU}(f_l^L(\mathcal{R}^{(\tau)}))}{C(l)} \right). \quad (5)$$

It is similar to the constraint loss but only considers final output of the algorithm. The *objective gap without constraint violation* (**OnoCGap**) is the objective gap when the solution is scaled by the maximum ratio of constraint violation, thereby ensuring the final solution is feasible. Finally, the *training time* per epoch and the *prediction time* measure the time spent on training for each epoch on average, and the time for making each prediction on average during testing (or running IPM on one instance till optimality for SciPy), respectively.

D. Evaluation Results

TABLE II: **OnoCGap** (%) for HARP, TEAL and TELGEN

OnoCGap (%)	HARP	TEAL	TELGEM
B4	26.99	26.21	2.99
ASN ₉₈	73.04	98.07	1.70
ASN ₅₁₀	3902.69	99.98	1.95

TABLE III: Model training time per epoch and prediction time per test instance

Training Time (second)	HARP	TEAL	TELGEM
B4	0.86	2.00	1.63
ASN ₉₈	12.59	7.80	2.56
ASN ₅₁₀	43251.11	127.96	2.64
Prediction Time (ms)	HARP	TEAL	TELGEM
B4	29.28	5.04	1.55
ASN ₉₈	814.27	4.5	1.52
ASN ₅₁₀	20474.78	358.10	1.53

1) *Comparing TELGEN, TEAL and HARP:* We first compared the performance of TELGEN to TEAL and HARP, the state-of-the-art learning-based TE solutions. Since TEAL needs to be trained and tested on the same network topology, while HARP cannot execute on the whole ASN graph, we evaluated all three algorithms by training and testing them on datasets generated on B4 and two connected sub-networks of ASN with 98 nodes and 202 edges, 510 nodes and 1600 edges denoted as ASN₉₈ and ASN₅₁₀, respectively.

Table II shows **OnoCGap**—objective gap when each solution was rounded to be feasible—of TELGEN, TEAL and HARP on the three datasets. First, we observe that TELGEN achieved negligible ($< 3\%$) objective gap, and the performance was consistent across topologies of different sizes. TELGEN strongly outperformed both TEAL and HARP, both of which had over 26% gap on B4, and over 73% gap on ASN datasets. We independently investigated the inferior performance of TEAL and HARP on our test sets. For TEAL, it was mainly because of the difference in traffic demands: TEAL’s original paper considered full traffic matrices with pairwise traffic demands, while our datasets included traffic demands only for randomly selected SD pairs. This led to TEAL inefficiently optimizing for many unnecessary SD pairs, showing its model’s inflexibility when facing diverse TE requirements. For HARP, the main reason was that it was designed for a different objective (MLU) than both TEAL and TELGEN, and could not be trivially modified to adopt a different objective due to its MLU-oriented model architecture. As such, its performance suffered when evaluated under the total flow objective since it unnecessarily constrained flows along non-bottlenecked paths.

In Table III, both TEAL and HARP showed comparable or faster **training time** per epoch as TELGEN on B4, but both became at least $3\times$ and $48\times$ slower than TELGEN when facing the larger ASN₉₈ and ASN₅₁₀ topologies. For **prediction time** when making a prediction, TELGEN again significantly outperformed TEAL by over $3\times$ for B4 and

TABLE IV: B4 and ASN: gaps (%) and prediction time (ms)

Dataset	Gaps (%)			Time (ms)	
	OGap	CGap	OnoCGap	TELGEN	SciPy
B4	6.40	3.97	2.99	1.55	9.41
ASN ₅₅₃ ^{test}	2.31	0.63	1.48	3.70	12.84
ASN ₁₇₃₉ ^{test}	2.41	0.18	2.01	3.73	11.43

ASN₉₈, 358× for ASN₅₁₀; HARP by over 18× for B4, 500× for ASN₉₈ and 13000× for ASN₅₁₀ due to its simple, fully GPU-compatible architecture.

Especially, we observe that TELGEN kept almost a *constant prediction time* when scaling to drastically different network sizes. TELGEN’s efficiency mainly comes from its efficient model design, and that it requires no classical post-processing during training and can be entire trained and executed on GPU. Further, TELGEN only processes SD pairs with actual traffic demands, significantly reducing its memory footprint and improving training and prediction efficiency. TEAL’s fairly complex model pipeline (combining GNN with MARL) and the need for the expensive ADMM post-processing contributed mainly to its inefficiency, especially since ADMM can only be run on CPU. HARP has a complex model architecture with set transformers and specially designed recurrent adjustment units (RAUs), which contributed to its slow training and prediction. Both TEAL and HARP also process full traffic matrices regardless of whether a pair of nodes have demands or not, further increasing memory footprint and slowing down training and prediction.

While the above results show TELGEN’s superior performance and efficiency compared to state-of-the-art algorithms when training and testing on the same topology, the next sets of experiments fully unveil TELGEN’s generalization power, for which *no existing learning-based TE solution can compare*. As a remark, while HARP also has some limited generalizability, it is hard to fairly compare TELGEN’s and HARP’s generalization power for two reasons: (1) their different objectives make their solutions not easily comparable, as shown in Table II; (2) HARP only adapts to up to 20% differences from the training topology as in [3], which is not comparable to the goal of TELGEN to generalize to totally unseen, potentially much larger topologies during testing compared to training. Therefore, we next compare TELGEN’s performance to the most generalizable baseline—the SciPy IPM solver itself.

2) *Generalization on Real-world Networks*: The results are shown in Table IV. For the two ASN test sets, note that the training set contained only two **much smaller subnetworks** of the entire network, with around 40% of the links as in ASN₅₅₃^{test} and 7% of the links as in ASN₁₇₃₉^{test}. Also note that the training set had **no overlap** in nodes or links with the ASN₅₅₃^{test} due to how we constructed the training and test sets. Nevertheless, we observe that TELGEN achieved almost negligible OGap (< 2.5%) and CGap (< 0.65%) in both test sets compared to the optimal solution output by IPM. After scaling, the OnoCGap was < 2.1%. The OnoCGap was *reduced* compared to OGap since TELGEN tended to

TABLE V: Gaps (%) for all ER test datasets

Dataset	OGap	CGap	OnoCGap
ER _{200,0.7} ^{test}	1.36	0.11	1.25
ER _{200,0.8} ^{test}	1.27	0.12	1.16
ER _{200,0.9} ^{test}	0.97	0.09	0.73
ER _{500,0.7} ^{test}	1.27	0.11	1.17
ER _{500,0.8} ^{test}	1.29	0.11	1.20
ER _{500,0.9} ^{test}	0.97	0.08	0.85
ER _{1000,0.7} ^{test}	1.21	0.10	1.13
ER _{1000,0.8} ^{test}	1.40	0.11	1.31
ER _{1000,0.9} ^{test}	0.97	0.07	0.90
ER _{2000,0.7} ^{test}	1.24	0.10	1.16
ER _{2000,0.8} ^{test}	1.27	0.11	1.20
ER _{2000,0.9} ^{test}	0.99	0.07	0.92

TABLE VI: Gaps (%) for all WA test datasets

Dataset	OGap	CGap	OnoCGap
WA ₂₀₀₀ ^{test}	2.08	0.46	1.10
WA ₃₀₀₀ ^{test}	2.16	0.47	1.16
WA ₄₀₀₀ ^{test}	2.21	0.46	1.20
WA ₅₀₀₀ ^{test}	3.70	0.62	1.89

“slightly over-provision”—allocating more than link capacities which led to (infeasibly) higher objective than the optimal solution—which was corrected after the solution was scaled down by capacity violation. This was precisely the behavior we wanted TELGEN to learn: to maximize the objective as the IPM algorithm did even when the “maximize” symbol itself was not encoded in the GNN inputs at all.

TELGEN achieved 16.5%-71.2% reduction in **prediction time** over SciPy. The advantage is expected to become larger with larger TE instances (e.g. larger networks and more SD pairs). In principle, TELGEN involves **linear complexity** in the number of variables while the fastest LP solver involves almost *cubic complexity*. Moreover, TELGEN can utilize massive parallelism enabled by GPU, while traditional solvers can at best perform CPU parallelism, further limiting scalability.

3) *Generalization on Random Topologies*: In random dataset experiments, we trained our TELGEN model on the 54 topology configurations for ER dataset and 7 topology configurations for WA dataset. The trained models had been tested on 12 test graphs with different number of nodes and probability for ER graphs while 4 test graphs with different number of nodes and β for WA graphs. Table V and VI show test datasets with detailed node numbers and/or link generation parameters, as well as OGap, CGap and OnoCGap achieved for each test dataset. For both ER and WA datasets, TELGEN achieved negligible objective and constraint gaps, and the OnoCGap was below < 2% for all test sets. The increase in network sizes in the test datasets led to negligible impact on the gaps as well, demonstrating **strong generalizability** of

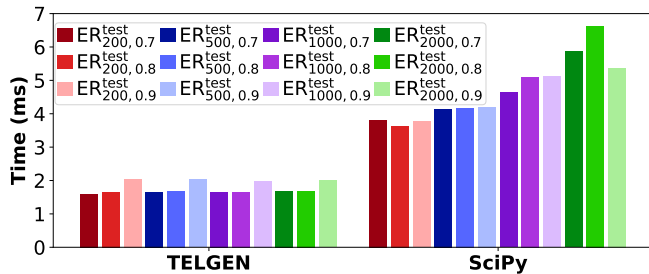


Fig. 3: Prediction time for different ER test datasets based on number of nodes and edge probability

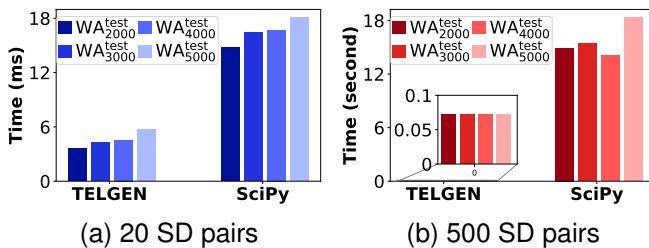


Fig. 4: Prediction time for different WA test datasets based on number of nodes and different number of SD pairs

TELGEN even when the test networks had 2-20 \times more nodes than the largest training networks. The WA test set witnessed slightly larger gaps when the network became very larger with 6 \times more nodes than training, but the result was still superior.

For **prediction time** of generating a solution, Figs. 3 and 4 show that TELGEN again outperformed the traditional SciPy solver by over 3 \times for ER and WA test graphs. The more nodes or links the graph had, the more time TELGEN spent to make one prediction as observed in the figures. The advantage of TELGEN enlarged when the problem size—the number of SD pairs—increased as in Fig. 4(b). When the SD pair number went up to 500, TELGEN sped up the traditional SciPy solver by over 200 \times , validating the asymptotic advantage (linear vs. cubic) and demonstrating significant efficiency improvement for large-scale problems.

4) *Generalization to Unseen Demand Distributions*: Finally, we show TELGEN’s generalization power when given different ranges of demands than seen during training. We changed the demand range by 20% over the original range of [1000, 5000], leading to two demand ranges: [1200, 6000] and [800, 4000]. We tested the different demand ranges on the ER test datasets with a 0.9 connection probability. Detailed information is shown in Table VII. TELGEN again achieved negligible gaps compared to the optimal solution given either larger or smaller demands than training, with the OnoCGap < 3% for the former and < 0.8% for the latter. The slightly higher gaps with higher demands were due to the link capacities being more saturated.

Remarks: Based on the results, we believe TELGEN can be particularly beneficial in two scenarios: (1) A **network operator** of a large-scale network can train and evaluate a TELGEN model on smaller subnetworks, such as within a

TABLE VII: ER Gaps (%) with unseen demand distributions

Dataset	Demand range	OGap	CGap	OnoCGap
ER _{200,0.9} ^{test}	[1200, 6000]	2.98	0.13	2.74
ER _{500,0.9} ^{test}	[1200, 6000]	3.09	0.13	2.89
ER _{1000,0.9} ^{test}	[1200, 6000]	2.66	0.13	2.45
ER _{2000,0.9} ^{test}	[1200, 6000]	2.94	0.13	2.73
ER _{200,0.9} ^{test}	[800, 4000]	0.75	0.09	0.71
ER _{500,0.9} ^{test}	[800, 4000]	0.79	0.09	0.75
ER _{1000,0.9} ^{test}	[800, 4000]	0.70	0.09	0.67
ER _{2000,0.9} ^{test}	[800, 4000]	0.75	0.09	0.71

region, and then generalize the pre-trained model to the entire WAN without expensive re-training. This can enable very efficient training than using the entire network topology for training. (2) A **networking software provider** can train general TE models using small known or random topologies, and ship these models as part of their software to operators. The operators need zero or minimal fine-tuning to generalize these models onto their own, heterogeneous large-scale networks.

VI. CONCLUSIONS

This paper introduced an innovative methodology for designing customized graph deep learning models and learning algorithms, to tackle the challenges of large-scale network TE problems and ensure generalization to diverse network configurations. TELGEN, a learning-based TE framework, was designed to efficiently solve large-scale TE problems with generalizability. By capturing the relationships among problem variables, objectives, and constraints, TELGEN makes predictions on the TE solution based on a structured graph representation of each problem instance. Two key components for enabled TELGEN’s strong generalization include: flexible model architecture that allows training on diverse topologies, and strong supervision from the classical IPM algorithm for learning instance-agnostic optimization processes.

To evaluate its performance, we trained and tested TELGEN on large-scale randomly generated and real-world network topologies. Extensive experiments demonstrated that TELGEN can solve large-scale TE problems close to optimality, improves prediction time by multiple folds compared to the optimal TE solver, significantly reduces training time on large networks over state-of-the-art learning-based solutions. More importantly, TELGEN generalizes seamlessly to unseen large-scale networks with pre-training on much smaller networks and synthetic traffic demands. With its superior performance and generalizability, TELGEN has the potential to serve as a fundamental building block towards a general-purpose, fully automated software suite for managing large-scale computer networks.

REFERENCES

- [1] (1999) The caida ucscd [as relationships]. URL: <https://catalog.caida.org/dataset/as-relationships/>

- [2] F. Abuzaid, S. Kandula, B. Arzani, I. Menache, M. Zaharia, and P. Bailis, “Contracting wide-area network topologies to solve flow problems quickly,” in *USENIX NSDI*, 2021, pp. 175–200.
- [3] A. A. AlQiam, Y. Yao, Z. Wang, S. S. Ahuja, Y. Zhang, S. G. Rao, B. Ribeiro, and M. Tawarmalani, “Transferable neural wan te for changing topologies,” in *ACM SIGCOMM*, 2024.
- [4] G. Bernárdez, J. Suárez-Varela, A. López, B. Wu, S. Xiao, X. Cheng, P. Barlet-Ros, and A. Cabellos-Aparicio, “Is machine learning ready for traffic engineering optimization?” in *IEEE ICNP*, 2021, pp. 1–11.
- [5] Q. Cappart, D. Chételat, E. B. Khalil, A. Lodi, C. Morris, and P. Veličković, “Combinatorial optimization and reasoning with graph neural networks,” *Journal of Machine Learning Research*, vol. 24, no. 130, pp. 1–61, 2023.
- [6] Z. Chen, J. Liu, X. Wang, J. Lu, and W. Yin, “On representing linear programs by graph neural networks,” *arXiv*, 2022.
- [7] chendiqian. Ipm-gnn: Exploring the power of graph neural networks in solving linear optimization problems. URL: https://github.com/chendiqian/IPM_MPNN.git
- [8] T. S. community. Scipy documentation. URL: <https://docs.scipy.org/doc/scipy/reference/generated/scipy.optimize.linprog.html>
- [9] D. Eppstein, “Finding the k shortest paths,” *SIAM Journal on Computing*, vol. 28, no. 2, pp. 652–673, 1998.
- [10] L. Erdős, A. Knowles, H.-T. Yau, and J. Yin, “Spectral statistics of erdős-rényi graphs i: Local semicircle law,” *IMS The Annals of Probability*, no. 3B, pp. 2279–2375, 2013.
- [11] M. Ferriol-Galmés, J. Paillisse, J. Suárez-Varela, K. Rusek, S. Xiao, X. Shi, X. Cheng, P. Barlet-Ros, and A. Cabellos-Aparicio, “Routenet-fermi: Network modeling with graph neural networks,” *IEEE/ACM Transactions on Networking*, vol. 31, no. 6, pp. 3080–3095, 2023.
- [12] M. Ferriol-Galmés, K. Rusek, J. Suárez-Varela, S. Xiao, X. Shi, X. Cheng, B. Wu, P. Barlet-Ros, and A. Cabellos-Aparicio, “Routenet-erlang: A graph neural network for network performance evaluation,” in *IEEE INFOCOM*, 2022, pp. 2018–2027.
- [13] L. K. Fleischer, “Approximating fractional multicommodity flow independent of the number of commodities,” *SIAM Journal on Discrete Mathematics*, vol. 13, no. 4, pp. 505–520, 2000.
- [14] V. Garg, S. Jegelka, and T. Jaakkola, “Generalization and representational limits of graph neural networks,” in *ICML*. PMLR, 2020, pp. 3419–3430.
- [15] J. Gondzio, “Interior point methods 25 years later,” *European Journal of Operational Research*, vol. 218, no. 3, pp. 587–601, 2012.
- [16] L. Gurobi Optimization. Gurobi optimizer reference manual. URL: <https://www.gurobi.com/documentation/current/refman/index.html>
- [17] IBM. Ibm ilog cplex optimization studio. URL: <https://www.ibm.com/products/ilog-cplex-optimization-studio>
- [18] S. Jain, A. Kumar, S. Mandal, J. Ong, L. Poutievski, A. Singh, S. Venkata, J. Wanderer, J. Zhou, M. Zhu *et al.*, “B4: Experience with a globally-deployed software defined wan,” *ACM SIGCOMM*, vol. 43, no. 4, pp. 3–14, 2013.
- [19] C. K. Joshi, T. Laurent, and X. Bresson, “An efficient graph convolutional network technique for the travelling salesman problem,” *arXiv*, 2019.
- [20] M. Lee, S. Hosseinipour, C. G. Brinton, G. Yu, and H. Dai, “A fast graph neural network-based method for winner determination in multi-unit combinatorial auctions,” *IEEE Transactions on Cloud Computing*, vol. 10, no. 4, pp. 2264–2280, 2020.
- [21] Z. Li, Q. Chen, and V. Koltun, “Combinatorial optimization with graph convolutional networks and guided tree search,” *NeurIPS*, vol. 31, 2018.
- [22] L. Liu, L. Chen, H. Xu, and H. Shao, “Automated traffic engineering in sdwan: Beyond reinforcement learning,” in *IEEE INFOCOM WKSHPS*, 2020, pp. 430–435.
- [23] X. Liu, S. Zhao, and Y. Cui, “Figret: Fine-grained robustness-enhanced traffic engineering,” *arXiv*, 2024.
- [24] Z. Liu, Z. Wang, X. Yin, X. Shi, Y. Guo, and Y. Tian, “Traffic matrix prediction based on deep learning for dynamic traffic engineering,” in *IEEE ISCC*, 2019, pp. 1–7.
- [25] ———, “Traffic matrix prediction based on deep learning for dynamic traffic engineering,” in *IEEE ISCC*, 2019, pp. 1–7.
- [26] A. Mendiola, J. Astorga, E. Jacob, and M. Higuero, “A survey on the contributions of software-defined networking to traffic engineering,” *IEEE Communications Surveys & Tutorials*, vol. 19, no. 2, pp. 918–953, 2016.
- [27] D. Narayanan, F. Kazhamiaka, F. Abuzaid, P. Kraft, A. Agrawal, S. Kandula, S. Boyd, and M. Zaharia, “Solving large-scale granular resource allocation problems efficiently with pop,” in *ACM SIGOPS*, 2021, pp. 521–537.
- [28] J. Nocedal and S. J. Wright, *Numerical optimization*. Springer, 1999.
- [29] T. Pan, X. Peng, Z. Bian, X. Lin, E. Song, and T. Huang, “Power-aware traffic engineering via deep reinforcement learning,” in *IEEE INFOCOM WKSHPS*, 2019, pp. 1009–1010.
- [30] Y. Perry, F. V. Frujeri, C. Hoch, S. Kandula, I. Menache, M. Schapira, and A. Tamar, “Dote: Rethinking (predictive) wan traffic engineering,” in *USENIX NSDI*, 2023, pp. 1557–1581.
- [31] P. Pinyoanuntapong, M. Lee, and P. Wang, “Delay-optimal traffic engineering through multi-agent reinforcement learning,” in *IEEE INFOCOM WKSHPS*, 2019, pp. 435–442.
- [32] C. Qian, D. Chételat, and C. Morris, “Exploring the power of graph neural networks in solving linear optimization problems,” in *AISTATS*. PMLR, 2024, pp. 1432–1440.
- [33] K. Sattar, F. Chikh Oughali, K. Assi, N. Ratrou, A. Jamal, and S. Masiur Rahman, “Transparent deep machine learning framework for predicting traffic crash severity,” *Neural Computing and Applications*, vol. 35, no. 2, pp. 1535–1547, 2023.
- [34] P. Virtanen, R. Gommers, T. E. Oliphant, M. Haberland, T. Reddy, D. Cournapeau, E. Burovski, P. Peterson, W. Weckesser, J. Bright, S. J. van der Walt, M. Brett, J. Wilson, K. J. Millman, N. Mayorov, A. R. J. Nelson, E. Jones, R. Kern, E. Larson, C. J. Carey, Í. Polat, Y. Feng, E. W. Moore, J. VanderPlas, D. Laxalde, J. Perktold, R. Cimrman, I. Henriksen, E. A. Quintero, C. R. Harris, A. M. Archibald, A. H. Ribeiro, F. Pedregosa, P. van Mulbregt, and SciPy 1.0 Contributors, “SciPy 1.0: Fundamental Algorithms for Scientific Computing in Python,” *Nature Methods*, vol. 17, pp. 261–272, 2020.
- [35] P. Wang, S.-C. Lin, and M. Luo, “A framework for qos-aware traffic classification using semi-supervised machine learning in sdn,” in *IEEE SCC*, 2016, pp. 760–765.
- [36] B. M. Waxman, “Routing of multipoint connections,” *IEEE Journal on Selected Areas in Communications*, vol. 6, no. 9, pp. 1617–1622, 1988.
- [37] Z. Wu, S. Pan, F. Chen, G. Long, C. Zhang, and S. Y. Philip, “A comprehensive survey on graph neural networks,” *IEEE Transactions on Neural Networks and Learning Systems*, vol. 32, no. 1, pp. 4–24, 2020.
- [38] K. Xu, J. Li, M. Zhang, S. S. Du, K.-i. Kawarabayashi, and S. Jegelka, “What can neural networks reason about?” *arXiv*, 2019.
- [39] Z. Xu, F. Y. Yan, R. Singh, J. T. Chiu, A. M. Rush, and M. Yu, “Teal: Learning-accelerated optimization of wan traffic engineering,” in *ACM SIGCOMM*, 2023, pp. 378–393.
- [40] G. Zarpellon, J. Jo, A. Lodi, and Y. Bengio, “Parameterizing branch-and-bound search trees to learn branching policies,” in *AAAI*, vol. 35, no. 5, 2021, pp. 3931–3939.
- [41] J. Zhang, Z. Guo, M. Ye, and H. J. Chao, “Smartentry: Mitigating routing update overhead with reinforcement learning for traffic engineering,” in *ACM NetAI*, 2020, pp. 1–7.

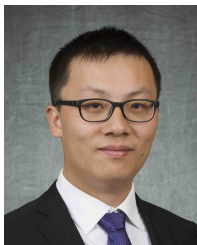


Fangtong Zhou (Student Member 2021) received her B.E. degree (2018) in Electrical Engineering and Automation from Harbin Institute of Technology, Harbin, China and M.S. degree (2020) in Electrical Engineering from Texas A&M University, College Station, Texas, USA. Currently she is a Ph.D candidate in the School of Computer Science at North Carolina State University. Her research interests include machine learning in computer networking, like federated learning, reinforcement learning for resource provisioning, etc.



Xiaorui Liu (Member 2023) is an Assistant Professor of Computer Science at North Carolina State University (USA). He earned his PhD degree in Computer Science from Michigan State University (USA) in 2022. His research focuses on graph deep learning, trustworthy artificial intelligence, and large-scale machine learning. He is the recipient of AAAI New Faculty Highlights (2025), National AI Research Resource Pilot Award (2024), ACM SIGKDD Outstanding Dissertation Award (Runner-up, 2023), Amazon Research Award (2023), and

Chinese Government Award for Outstanding Students Abroad (2022). He has served on the Organizing Committee of ACM SIGKDD as a Workshop Chair and as a regular Program Committee member of conferences including ICML, ICLR, NeurIPS, and KDD.



Ruozhou Yu (Student Member 2013, Member 2019, Senior Member 2021) is an Assistant Professor of Computer Science at North Carolina State University, USA. He received his PhD degree (2019) in Computer Science from Arizona State University, USA. His research interests include network optimization, cloud/edge computing, security and privacy, blockchain, quantum networks, and satellite networks. He has served on the organizing committee of IEEE INFOCOM 2022-2025, IEEE IPCCC 2020-2024 and IEEE QCNC 2024, as a Track Chair

for IEEE ICCCN 2023, and as members of the technical committee of IEEE INFOCOM 2020-2025, ACM Mobihoc 2023-2025 and IEEE ICDCS 2025. He is an Area Editor of Elsevier Computer Networks, and an Associate Editor of IEEE Transactions on Network Science and Engineering. He is a recipient of the NSF CAREER Award in 2021.



Guoliang Xue (Member 1996, Senior Member 1999, Fellow 2011) is a Professor of Computer Science in the School of Computing and Augmented Intelligence at Arizona State University. His research interests span the areas of Internet-of-things, cloud/edge/quantum computing and networking, crowdsourcing and truth discovery, QoS provisioning and network optimization, security and privacy, optimization and machine learning. He received the IEEE Communications Society William R. Bennett Prize in 2019. He is an Associate Editor

of IEEE Transactions on Mobile Computing, as well as a member of the Steering Committee of this journal. He served on the editorial boards of IEEE/ACM Transactions on Networking and IEEE Network Magazine, as well as the Area Editor of IEEE Transactions on Wireless Communications, overseeing 13 editors in the Wireless Networking area. He has served as VP-Conferences of the IEEE Communications Society. He is the Steering Committee Chair of IEEE INFOCOM.

VII. APPENDIX

A. MLU Optimization Problem Formulation

Traffic Splitting. The basic TE problem has decision variables, defined as *traffic splitting ratios* \mathcal{R} , which denote allocated fractions of each SD pair's demand to possible paths of the SD pair. We define $\mathcal{R}(p)$ as the fraction of the demand d_i that is allocated to path $p \in P_i$. The total traffic split ratio of an SD pair cannot exceed 100%. We thus represent the variables as a mapping $\mathcal{R} : P \rightarrow [0, 1]$, and enforce this constraint in the formulation as described below. We use α to represent the MLU variable.

Objective. The basic goal of MLU optimization is to minimize the maximum link utilization. This lead to the objective function as: minimize α .

Constraints. The problem has two sets of constraints. First, the total allocated traffic for each SD pair cannot exceed its demand, and hence $\sum_{p \in P_i} \mathcal{R}(p) \leq 1$ for every $i \in D$. Second, the traffic allocated on a link cannot exceed its capacity multiplied by MLU, and hence we have $\sum_{i \in D} d_i \sum_{p \in P_i: l \in p} \mathcal{R}(p) \leq \alpha \cdot C(l)$ for $\forall l \in L$.

TE Optimization. We formulate TE optimization as:

$$\begin{aligned}
 & \text{minimize} && \alpha \\
 & \text{subject to} && \sum_{p \in P_i} \mathcal{R}(p) \leq 1, \quad \forall i \in D; \\
 & && \sum_{i \in D} d_i \sum_{p \in P_i: l \in p} \mathcal{R}(p) \leq \alpha \cdot C(l), \quad \forall l \in L; \quad (6) \\
 & && \mathcal{R}(p) \geq 0, \quad \forall p \in P; \\
 & && \alpha \geq 0.
 \end{aligned}$$

For simplicity, we define constraint functions $f_i^D(\mathcal{R}) \triangleq \sum_{p \in P_i} \mathcal{R}(p) - 1$, and $f_l^L(\mathcal{R}) \triangleq \sum_{i \in D} d_i \sum_{p \in P_i: l \in p} \mathcal{R}(p) - C(l)$. We want to design an algorithm that solves (6) to its optimality, ensures feasibility of the solution, and can do so efficiently on very large network scenarios (with thousands of nodes) even on those not observed in the training process.